J Nanopart Res (2014) 16:2515
DOI 10.1007/s11051-014-2515-y

RESEARCH PAPER

Nanoengineered mesoporous silica nanoparticles for smart delivery of doxorubicin

Akhilesh Kumar Mishra · Himanshu Pandey · Vishnu Agarwal · Pramod W. Ramteke · Avinash C. Pandey

Received: 22 January 2014 / Accepted: 10 June 2014 / Published online: 3 July 2014

Abstract The motive of the at hand exploration was to contrive a proficient innovative pH-responsive nanocarrier designed for an anti-neoplastic agent that not only owns competent loading capacity but also talented to liberate the drug at the specific site. pH sensitive hollow mesoporous silica nanoparticles (∼MSN) have been synthesized by sequence of chemical reconstruction with an average particle size of 120 nm. ∼MSN reveal noteworthy biocompatibility and efficient drug loading magnitude. Active molecules such as Doxorubicin (DOX) can be stocked and set free from the pore vacuities of ∼MSN by tuning the pH of the medium. The loading extent of ∼MSN was found up to 81.4 wt% at pH 7.8. At mild acidic pH, DOX is steadily released from the pores of ∼MSN. Both, the nitrogen adsorption–desorption isotherms and X-ray diffraction patterns reflects that this system holds remarkable stable mesostructure. Additionally, the outcomes of cytotoxicity assessment further establish the potential of ∼MSN as a relevant drug transporter which can be thought over an appealing choice to a polymeric delivery system.

Keywords Mesoporous silica nanoparticles · Cytotoxicity assays · Doxorubicin hydrochloride · Drug delivery · Nanomedicine

A. K. Mishra (✉) · H. Pandey · P. W. Ramteke
Department of Pharmaceutical Sciences, Faculty of Health Sciences, Sam Higginbottom Institute of Agriculture, Technology & Sciences, Allahabad 211007, India
e-mail: akhileshmishra2010@gmail.com

A. K. Mishra · H. Pandey · A. C. Pandey
Nanotechnology Application Centre, Faculty of Science, University of Allahabad, Allahabad 211002, India

V. Agarwal
Department of Biotechnology, Motilal Nehru National Institute of Technology, Allahabad 211004, India

Introduction

In the recent decades, conspicuous progression in the groundwork of drug delivery has been made owing to their inordinate aptitude to ameliorate therapeutic demand of pharmacologically active molecules at the goal site, particularly in cancer therapy (Khaled et al. 2005; Tasciotti et al. 2008; Pandey et al. 2011). The most frequently used traditional dosage format has flaws, such as miserable solubility and biodistribution, swift clearance of the drug from desired location, tissue devastation on extravasation, and unspecific uptake of normal cells, that limits the desired pharmacological action of the drug candidate. These impediments can be worked out by bringing in a relevant delivery system that mends the pharmacokinetic criterions of the drug substance and supervises its release rate in response to internal or external stimuli.

To escort the sturdy tissues/organs such as kidney, liver, bone marrow, and heart from the noxious drugs

and to avert the denaturing of the drugs prior to arriving the aimed intracellular and intra nuclear terrains, the stimuli-responsive "SMART" drug delivery porters have been immensely designed (Besseling et al. 1998; Stuart et al. 2010; Tang et al. 2011; Carmen et al. 2013). These "SMART" drug-delivery systems are prone to a swift response toward the fluctuations of regional ambience, such as temperature (Schmaljohann 2006), pH (Liu and Eisenberg 2003; Liu et al. 2006; Liao et al. 2011), light (Qiu and Park 2001), redox-regulated nanovalves grounded on mesostructured thin films for release of luminescent molecules (Lai et al. 2003; Mal et al. 2003; Hernandez et al. 2004; Yoo and Pak 2013), and magnetic field (Medeiros et al. 2011). All of these materials are smart only because they are "*Specific and Measurable Agents to Reach the Target site*".

Mesoporous silica nanoparticles (MSN) hold illustrious vow for a diversity of implementations and have come out as vehicles or reservoirs in a wide assortment of domains such as drug delivery (Vallet-Regi et al. 2001; Mou et al. 2008; Slowing et al. 2008; Lee et al. 2010; Manzano and Vallet-Regi 2010), adsorption and heterogeneous catalysis (Rao et al. 1997; Lim et al. 1998; Chen et al. 2003; Pere-Quintanilla et al. 2007), Biosensors (Radu et al. 2004; Trewyn et al. 2007), etc. Attainments are continuous to optimize their porous parameters, such as enhancement of pore volume or pore size, with the aspiration of considerably progressing the storage magnitude of cargoes, or promoting the host–guest specific interaction for the premeditated objective.

Various approaches have been developed to synthesize pH-responsive MSN-based nanocarriers for drug delivery. A supramolecular system with pH-responsive nanovalves annexed to the surface of MSN was developed (Angelos et al. 2008; Zhao et al. 2010; Meng et al. 2010). Martinez-Manez illustrated a mesoporous material embodying functional moieties of polyalcohol and boronic acid groups, which enabled "open-close" of the system by restraining pH (Aznar et al. 2009). Yang et al. notified a smart pH-responsive drug carrier founded on carboxylic acid modified SBA-15 silica rods (Yang et al. 2005). Poly(acrylic acid) and poly(methacrylic acid) chains were additionally spliced onto the surface of MSN to serve as pH sensitive gatekeeper (Hong et al. 2009; Gao et al. 2009). In addition, Sun et al. (2010) affixed poly(2-diethylaminoethyl methacry-late) (PDEAEMA) shells onto the exterior surface of MSN via surface-initiated atom transfer radical polymerization (ATRP) to whip up a novel nanodevice with MSN cores as drug carriers and pH-responsive PDEAEMA shells as smart nanovalves.

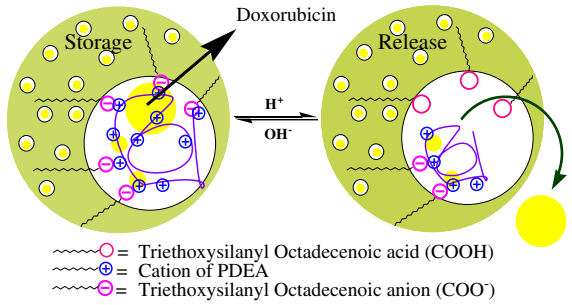

Fig. 1 Schematic representation of pH-responsive hollow mesoporous silica nanoparticles. The pH-controlled system is based on the interaction between negative carboxylic acid modified hollow mesoporous silica nanoparticles (CmMSN) with Polycations (PDEA)

Herein, we report smart pH-responsive carrier system (~MSN), based on interaction between carboxylic group of hollow mesoporous silica nanoparticles (CmMSN) and poly(2-diethylamino ethyl methacrylate) (PDEA), for the storage and smart release of drug molecules from pH sensitive orifice of the mesopores (Fig. 1).

Experimental section

Material

The entire chemical used in the study was of analytical grade. Cetyl trimethyl ammonium bromide (CTAB), Tetra ethyl orthosilicate (TEOS), and Poly(lactide-*co*-glycolides) (PLGA) were purchased from Scientific supplier (Gwalior, India). Doxorubicin in the form of its hydrochloride salt (DOX) was obtained from R.P.G. Life Sciences limited (Maharashtra, India). The entire reagents were used as purchased without further purification. Water used in the experiment was purified by Milli-Q system to a resistivity of 18.2 mΩ.cm.

Preparation of hollow mesoporous silica nanoparticles

Initially, the Poly(lactide co-glycolides) (PLGA) nanospheres were prepared by conventional emulsification/

solvent evaporation method (Park et al. 2003). The size of nanospheres is controlled by changing the molar ratio of PLGA, potassium persulfate (KPS), and CTAB. Hollow mesoporous silica nanoparticles (~MSN) were prepared using PLGA nanospheres as the core template and CTAB as structure-directing agent (Jiao et al. 2012). Briefly, 0.57 g of synthesized nanospheres having average diameter of 84 nm were dispersed uniformly in a mixed solution of ethanol (20 mL) and deionized water (50 mL). 10 mL of deionized water containing 0.3 g of CTAB was added. The mixture was stirred quickly for 30 min at 40 °C. Finally, 0.85 mL of aqueous ammonia solution (25 wt%) and 1.16 mL of tetraethyoxysilane (TEOS) were successively added to the above mixture. The reaction was carried out for 24 h. After several washing with water and ethanol, the products were refluxed in the ethanol solution of NH_4NO_3 (10 mg/mL) at 80 °C for 3 h to remove the surfactant (CTAB). The synthesized product was centrifuged and washed with ethanol three times and dried under vacuum (Yamato Vacuum Drying Oven, ADP200/300) at 150 °C for 3 h.

Synthesis of carboxylic acid modified hollow mesoporous silica nanoparticles (CmMSN)

CmMSN were prepared by functionalization of the surface of hollow mesoporous silica nanoparticles by triethoxysilanyl octadecenoic acid ethyl ester. Briefly, in 2 g of obtained dried sample of hollow mesoporous silica nanoparticles, 20 mL of dry toluene and 0.35 g of triethoxysilanyl octadecenoic acid ethyl ester were added and stirring at room temperature for 15 min. Toluene was evaporated by a rotary evaporator at 80 °C for 2 h, and the resulting material was dried under vacuum at 150 °C for 12 h. The obtained sample was placed in a round-bottom flask containing a bar magnetic stirring, equipped with a reflux condenser under nitrogen, followed by addition of dry CH_3CN (60 mL) and AlI_3 (0.2 g). After heating at 85 °C for 4 h, the mixture was cooled to ambient temperature, followed by filtration, washing with fresh Acetonitrile, and stirring with 10 % HCl for 1 h. After filtration, washing, and drying at room temperature for 24 h, carboxylic acid modified mesoporous silica nanoparticles were obtained.

pH-Controlled drug storage-release study

DOX was dissolved in distilled water at a concentration of 1 mg/mL. CmMSN (5 mg) were ultrasonically dispersed in 1 ml of the DOX solution. The mixture was stirred at room temperature for 24 h. After addition of PDEA (5 wt% in water, 2.5 mg), the pH value of the solution was adjusted to 7.8, and the solution was stirred for 3 h at room temperature. After filtration, washing with water three times for removal of DOX outside of mesopores and drying under vacuum at room temperature for 4 h, the DOX-loaded sample (DOX@MSN) was obtained. In comparison, another sample was prepared in the absence of PDEA. The mass of DOX loaded in the synthesized nanoparticles was analyzed by UV–Vis at a wavelength of 480 nm. The drug loading content and entrapment efficiency were calculated using the Eqs. (1) and (2), respectively (Tang et al. 2011; Jiao et al. 2012).

$$\text{Loading content } (\%) = \frac{\text{Initial amount of DOX} - \text{supernatant free amount of DOX}}{\text{DOX loaded composite nanospheres}} \times 100 \quad (1)$$

$$\text{Entrapment efficiency } (\%) = \frac{\text{Initial amount of DOX} - \text{supernatant free amount of DOX}}{\text{initial amount of drug}} \times 100 \quad (2)$$

A series of DOX-loaded sample were, respectively, dispersed in 2 mL of phosphate buffer saline (PBS) solutions of different pH values (2.0 and 6.5), and the samples were transferred into dialysis bags (molecular weight cut off 5,000). Then, the dialysis bags were kept in a 250-mL lucifugal sink with 200 mL of PBS (pH 2.0 or 6.5) and gently stirred at 37 °C. At timed intervals, 2 mL of the solution was extracted periodically, and then 2 mL of fresh PBS was added to keep the volume constant. The amount of released drug was analyzed by UV–Vis, and all released results were averaged over three measurements

Characterization

Nanoparticles size distribution (polydispersity index) and zeta potential (ζ) were determined using photon

correlation spectroscopy (Zetasizer, Beckman Coulter Inc., Delsa Nano 4C). The size distribution analysis was performed at a scattering angle of 90° and at a temperature of 25 °C using samples appropriately diluted with filtered water (0.2 μm filter; Minisart, Germany), whereas zeta potential was measured using a disposable zeta cuvette. All measurements were performed in triplicate ($n = 3$), and the standard deviation (SD) was recorded. The entrapment efficiency of ~MSN was determined by the separation of drug-loaded nanospheres from the aqueous medium containing non-associated DOX by ultracentrifugation (REMI high speed, cooling centrifuge, REMI Corporation, India) at 20,000 rpm at 4 °C for 30 min. The amount of DOX encapsulated into the nanospheres was calculated as the difference between the total amounts used to prepare the nanospheres and the amount that was found in the supernatant. The amount of free DOX in the supernatant was measured spectrophotometrically at 480 nm. UV–Vis spectra were obtained using a Perkin-Elmer Lambda 35 spectrophotometer. Modified nanosperes were visualized using a JEOL 6700F ultra high resolution scanning electron microscope (SEM). Fourier transform infrared spectroscopy (FTIR) measurements were performed with a Nicolet Impact 410 FT-IR spectrometer. A total of 2 % (w/w) of sample, with respect to the potassium bromide (KBr; S.D. Fine Chem. Ltd., Mumbai, India) disk, were mixed with dry KBr. The mixture was ground into fine powder using an agate mortar before compressing into KBr disk under a hydraulic press at 10,000 psi. Each KBr disk was scanned at 4 mm/s at resolution of 2 cm over a wave number region of 400–4,000 cm^{-1} using IR solution software (ver. 1.10). The characteristic peaks were recorded for different samples. Thermo gravimetric analysis (TGA) was used to measures the amount and rate of change in the weight of a material as a function of temperature in a controlled atmosphere. TGA thermograms of different samples were obtained using an automatic thermal analyzer system (Diamond TG/DTA 8.0, Perkin-Elmer, USA). Samples were crimped in standard aluminum pans and heated from 100 to 800 °C at a heating rate of 10 °C/min under constant purging of dry nitrogen at 20 ml/min. An empty pan, sealed in the same way as the sample, was used as a reference. X-ray diffraction (XRD) patterns were obtained with a Siemens D 5005 diffractometer using Cu Kα radiation. Nitrogen adsorption–desorption isotherms were obtained on a Micromeritics Tristar 3000 pore analyzer at 77 K under continuous adsorption conditions.

Cytotoxicity assays

A human cervical cancer cell line (HeLa cells) was used to evaluate the cytotoxicity of ~MSN and DOX@ ~MSN. HeLa cells were cultured in a RPMI-1640 medium supplemented with 10 % (v/v) fetal bovine serum, 2 mM L-glutamine, 100 U/mL penicillin, and 100 U/mL streptomycin at 37 °C and 5 % CO_2. The cytotoxicity was assessed using MTT (3-(4,5-dimethylthiazol-2-yl)-2,5-diphenyltetra-zolium bromide) assay. Cells were seeded into 96-well microtiter plates at the density of 20,000 cells per well. After incubation for 24 h, the medium was aspirated, and various concentrations of samples (free DOX and DOX@ ~MSN) in fresh cell growth medium were added. Control cells were added with equivalent volume of fresh media. Cells were cultured for 24 h before the cell viability assay was performed. The old medium was removed, and 100 μL of fresh medium and 10 μL of a 5-mg/mL MTT solution were added to each well. Plates were then incubated under cell culture conditions for 4 h. The old medium was aspirated, and 100 μL DMSO was added to dissolve the formazan crystals. The absorbance of each sample was measured at 570 nm.

Result and discussion

Preparation and characterization of CmMSN

As describe in experimental section, the sample is prepared by grafting of triethoxysilanyl Octadecenoic acid ethyl ester with the synthesized hollow mesoporous silica nanoparticles, refluxing in CH_3CN in the presence of AlI_3, and heating at 80 °C in ethanol. After interaction between surface silanol of mesoporous silica naoparticles with triethoxysilanyl Octadecenoic acid ethyl ester, the acid ethyl ester species attached on the pore outlets of as-synthesized CmMSN, as evidenced by an IR band at 1,735 cm^{-1} assigned to C=O species of ether (Fig. 2a). After refluxing in CH_3CN and AlI_{-3}, a new band at 1,712 cm^{-1} appears, which is associated with C=O species of the acid (Fig. 2b). These results indicate that the acid ethyl

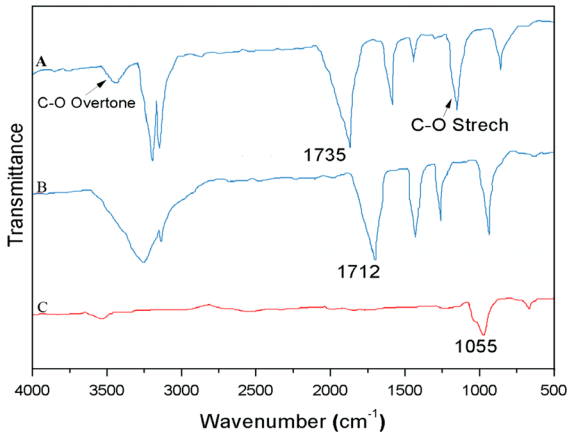

Fig. 2 FT-IR spectra of carboxylic acid modified mesoporous silica nanoparticles (CmMSN). (*a*) C=O of ether, (*b*) C=O of acid, and (*c*) hollow mesoporous silica nanoparticles

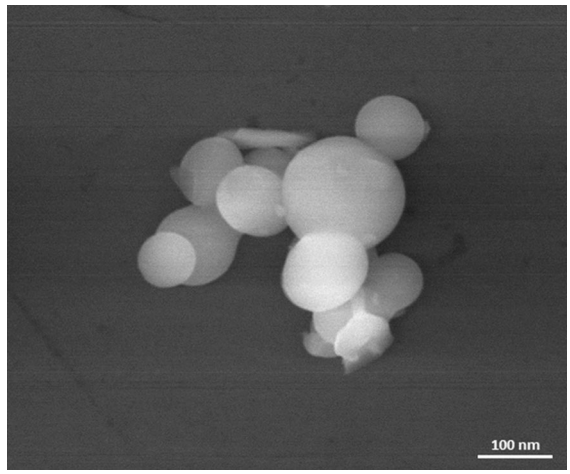

Fig. 3 SEM micrograph of carboxylic acid modified mesoporous silica nanoparticles (CmMSN)

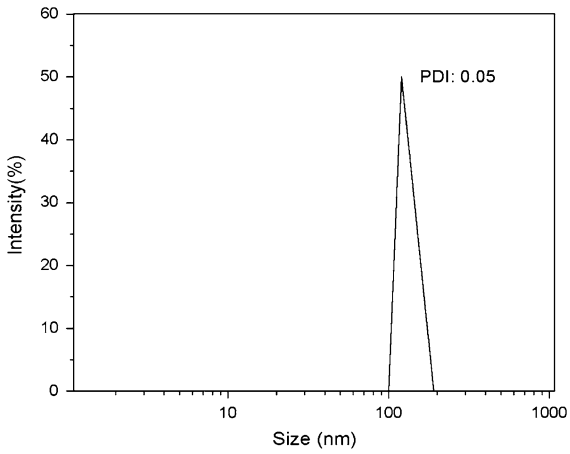

Fig. 4 DLS curve of carboxylic acid modified mesoporous silica nanoparticles (CmMSN)

ester groups modified on as-synthesized CmMSN are cleaved to carboxylic acidic groups. Hollow mesoporous silica nanoparticles show much simpler IR spectra (Fig. 2c). The main peak appears at 1,055 cm^{-1} due to the Si–O stretching vibration which implies that CTAB and PLGA are completely removed. Finally, CmMSN with a large amount of core volume are successfully prepared. Scanning electron microscopy image (Fig. 3) of sample shows the poly-dispersed hollow core with average diameter of about 120 nm. The polydispersity index (Fig. 4) of these CmMSN is approximately 0.05, suggesting a high size uniformity in these products measured by dynamic light scattering (DLS). As a typical guest molecule, DOX is used to study the efficiency of this pH-responsive carrier system. After the PDEA solution is mixed with the carboxylic acid modified hollow mesoporous silica nanoparticles and DOX, the drug-loaded sample (DOX@ ~MSN) is obtained. Nitrogen adsorption–desorption isothems (Fig. 5) also provide direct evidences of storage-release efficacy of the pH-controlled carrier system and indicative of a mesoporous character of ~MSN. Sample exhibits a typical type IV isotherm, giving a large pore volume (1.07 $cm^3\ g^{-1}$), surface area 962 $m^2\ g^{-1}$, and narrow pore size 2.7 nm, calculated by the Barret-Joyner-Halenda (BJH) method (Fig. 6). After loading of DOX, Nitrogen adsorption–desorption isothems still shows a type IV isotherm, but its pore volume (0.53 $cm^3\ g^{-1}$), surface area (467 $m^2\ g^{-1}$), and pore size distribution (1.9 nm) are drastically decreased, which should be attributed directly to DOX stored in the hollow core of the sample. Very interestingly, after DOX has been released, the sample still shows a typical IV isotherm, and its pore volume (0.83 $cm^3\ g^{-1}$), surface area (916 $m^2\ g^{-1}$), and pore size (2.7 nm) are obtained. All results mentioned above further demonstrate that this system is efficient for storage and release of DOX, and the mesostructure in this system is stable for drug delivery.

Figure 7, thermogravimetric analysis (TGA) was used to evaluate the organic residue in the resulting CmMSN. The CmMSN without the template removed give a weight loss of up to 43.2 % as a result of the

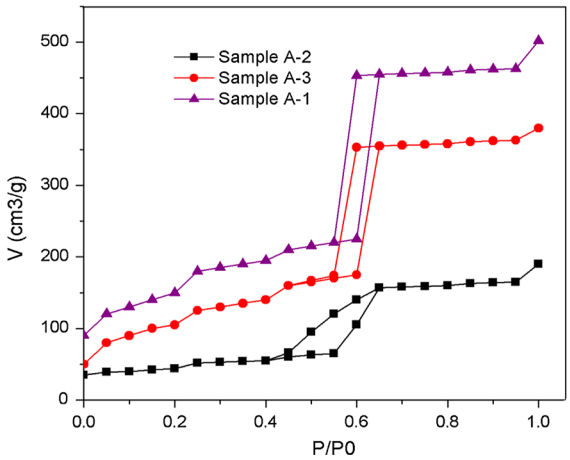

Fig. 5 Nitrogen adsorption/desorption isotherm of sample A-1 (~MSN before drug loading), A-2 (~MSN after drug loading), and A-3 (~MSN after drug release)

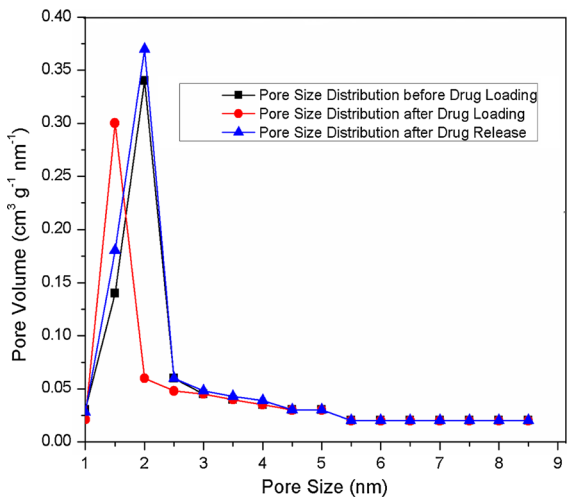

Fig. 6 Pore size distribution of pH sensitive hollow mesoporous silica nanoparticles (~MSN) obtained by BJH method

presence of the PLGA and CTAB templates. Upon treatment with the ethanol solution of NH_4NO_3 for 30 min, the obtained particles show a weight loss of 14.2 %, and when the processing time was prolonged by 6 h, their weight loss is just 13.3 % which is almost invariant when compared with the former. The additional weight loss is attributed to the dehydroxylation of Si–OH groups. As a result, it is believed that the template removal process, wherein the PLGA cores are dissolved in the solution accompanied by the CTAB removal through ion exchange, can be very quickly completed within 30 min.

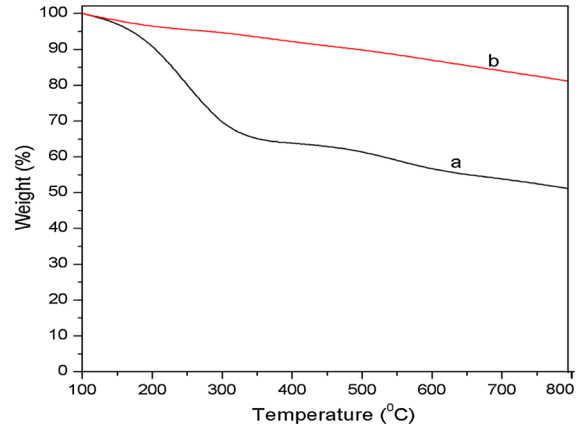

Fig. 7 TGA Thermogram of (*a*) CmMSN without the template removed (*b*) product collected after CmMSN was processed in the ethanol solution of NH_4NO_3 after 6 h

Effect of pH and ionic strength on the stability of the ~MSN

To investigate the pH-dependent behavior of the ~MSN, the pH values of the dispersed medium were changed from 3 to 8. Figure 8 exhibited the alteration tendency of zeta potentials and hydrodynamic diameters of ~MSN as a function of pH values. The trend of zeta potential showed a monotonous shape (Fig. 8b), while the hydrodynamic size showed a parabola shape (Fig. 8a) with pH variation. Similar results were demonstrated in the early report (Hu et al. 2005). Figure 8a demonstrated that the hydrodynamic size reached a minimum at pH 6.5. Above pH 4.0, the zeta potential was found to be negative, and the pH was higher than the *p*Ka of Octadecenoic acid. Below pH 4.0, the zeta potential got close to zero, and the repulsion among nanospheres was weaken leading to the aggregation of the nanospheres, so dramatic increase of the hydrodynamic diameter was observed. The above results were very important since it not only proved the pH-responsive property of ~MSN, but also indicated that the synthesized ~MSN were stable in the pH range of 5–8 and by controlling pH values, surface charges, and hydrodynamic size can be easily controlled, which are very important for their application in drug-delivery system.

Salt concentration also has a great influence on the stability of the ~MSN, so it is important to examine the stability of the modified nanospheres at different NaCl concentrations. In Table 1, it can be found that

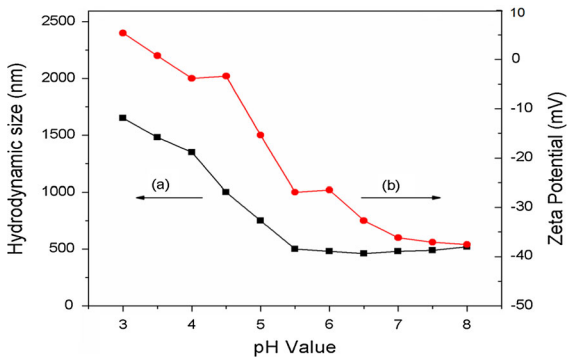

Fig. 8 The size (*a*) and zeta potential (*b*) of pH sensitive hollow mesoporous silica nanoparticles (~MSN) at different pH values

Table 1 Particle size and size distribution of hollow mesoporous silica nanoparticles at pH 7.4

NaCl concentration (mol/L)	Diameter[a] (nm)	PI[b]
0.10	180	0.04
0.20	180	0.04
0.30	183	0.08
0.60	184	0.06
1.00	189	0.1

[a] The diameter was determined at 25 °C by DLS

[b] *PI* polydispersity index, PI = $(\mu_2)/T^2$

the hydrodynamic diameters of the modified nanospheres just had a slight increase when the salt concentrations increased from 0.01 to 1.0 M. Above 0.60 M, the hydrodynamic diameters of the ~MSN increased rapidly together with the polydispersity indexes because more salt would screen the electrostatic charges on the surface of the carboxylic acid modified nanospheres (Stuart et al. 1998), leading to the destabilization of nanospheres. The useful conclusion was that the ~MSN were stable in the physiological saline (0.15 M NaCl) and were promising for the further application as drug vehicles.

DOX loading and release study

With the potential application in drug delivery, the CmMSN nanospheres were loaded with DOX for 24 h at 25 °C, and ultimately afforded DOX loading contents were found to be 18.4 ± 0.5 wt%, and their entrapment efficiencies were estimated to be 81.4 ± 2 wt%. To investigate pH-responsive release of this system, the DOX-loaded sample (DOX@ ~MSN) is

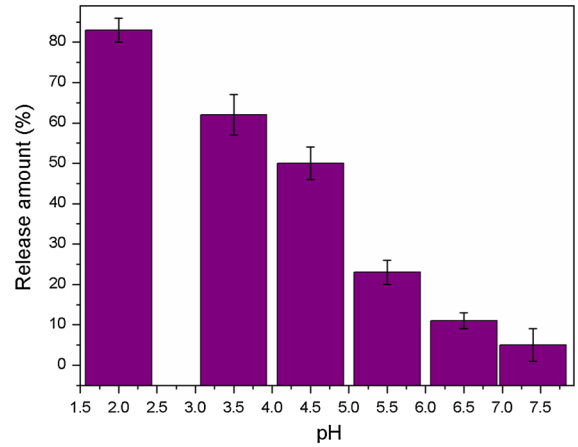

Fig. 9 Release amount of DOX from the sample at various pH values in 30 min

immersed in water at different pH values, and the mass transport from ~MSN to the solution was detected by UV spectrophotometer. Figure 9 shows the level of DOX released from sample at pH 2.0–pH 7.5 over the same time period (30 min). Obviously, the released amounts of DOX from ~MSN are stepwise from 8 to 86 % by adjusting the pH values from 7.4 to 2.0, which shows that the environment sensitive pores in the system are gradually opened. As shown in Fig. 1, polycations (PDEA) polymer binds to anionic CmMSN by oppositely charged ionic interaction and gate closed for storage of drugs in the mesopores. When ionized carboxylic acid species (COO^-) are transformed into unionized form (COOH) in acidic medium, polycations are separated from the surface of ~MSN, leading to opening of the mesopores for the release of drugs. Actually, interaction between polycations (PDEA) and anionic CmMSN is weakening with increasing acidity.

It is well known that the micro-environment around tumor tissues and other inflamed tissues in the body tends to be more acidic, relative to the normal tissues (pH 7.4). The release behaviors of ~MSN were tested at different pH values. As a control, the release curves of pure DOX solution in the dialysis bag at different pH values were determined first. The results show that the release trends of pure DOX in the dialysis bag at pH 2.0, 4.5, 6.5, and 7.4 have no distinct differences, and most of the DOX can be released in 1 h. So the dialysis bag did not interfere in the release trends of drug. Figure 10 shows the dependence of the released amount of DOX from the sample on time at pH values

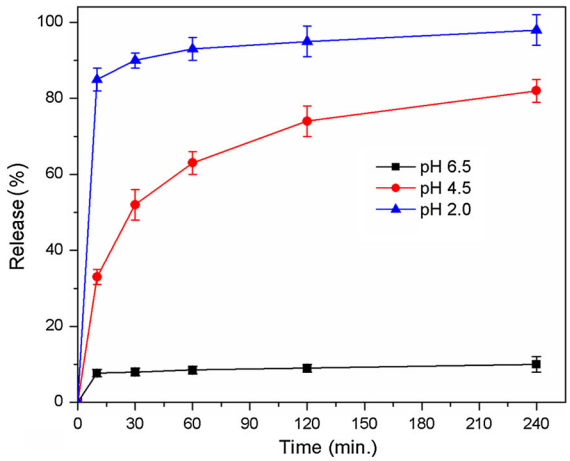

Fig. 10 Dependence of released amounts of DOX on time at different pH values

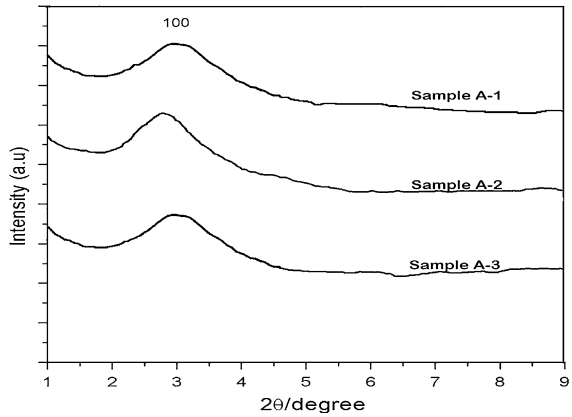

Fig. 11 XRD patterns of sample A-1 (~MSN before drug loading), sample A-2 (~MSN after drug loading), and sample A-3 (~MSN after drug release)

of 2.0, 4.5, and 6.5, respectively. Notably, the release rate is very fast at pH 2.0, and the amount basically reaches a maximum value of 90 wt% at 30 min possibly, in this case, there is not any negative charge on CmMSN. Therefore, PDEA with a positive charge will be separated from the surface of CmMSN, and then the state of the gates around the pores is completely opened. On the contrary, at pH 6.5, the release amount is quite low and remains essentially constant (10 wt%), which suggests that the state of the gates around the pores is almost closed due to a strong interaction between the negative group (COO^-) and the positive group of PDEA. It is very interesting to note that there is a steady release with stepwise increasing from 35.4 to 80.2 wt% during 4 h when at pH 4.5. This result indicates that drug delivery in our system at a mildly acidic pH value such as pH 4.5 may be long-lived and continuous, which is helpful for maintaining the concentration of drugs in the certain sites of the body within the optimum range.

XRD patterns

Figure 11 shows the XRD patterns of sample A-1 (~MSN before drug loading), A-2 (~MSN after drug loading), and A-3 (~MSN after drug release) for ~MSN, only a single broad peak was observed at 20°–30° confirming the formation of amorphous silica material. Obviously, these samples almost retain the same value and intensity of the d100 peaks, which indicates that DOX storage and release do not damage the ordered mesostructure in this system. It is well known that ordered mesoporous silica materials have good hydrothermal and chemical stability. Therefore, the carrier system based on the CmMSN will be considered an interesting alternative to the polymeric delivery system which suffers from limitations including poor thermal and chemical stability.

In-vitro cytotoxicity assays

The in-vitro cytotoxicity of ~MSN to HeLa cells was investigated by MTT assay. When the pure ~MSN were 0.1, 1, 10, and 100 μg/mL, the cell viabilities were 100 ± 5, 100 ± 5, 96 ± 5, and 96 ± 4 % for 24 h, respectively. The blank carrier (~MSN) showed no cytotoxicity on the HeLa cells even at the concentration of 100 μg/mL, this proves that the ~MSN carriers are biocompatible nanospheres. When the HeLa cells were treated with either the suspension of DOX@ ~MSN or a solution of pure DOX, significant decrease in the cancer cell viability was observed (Fig. 12). Furthermore, it was also seen that the DOX-loaded sample showed higher cytotoxicity than free DOX at the same dose. Also, the IC_{50} value (the concentration of drugs required to reduce cell growth by 50 %) for HeLa cells was determined to be 1.1 μg/mL for free DOX and 0.5 μg/mL for DOX@ ~MSN, respectively, so DOX@ ~MSN showed a more efficient cytotoxicity than pure DOX to HeLa cells.

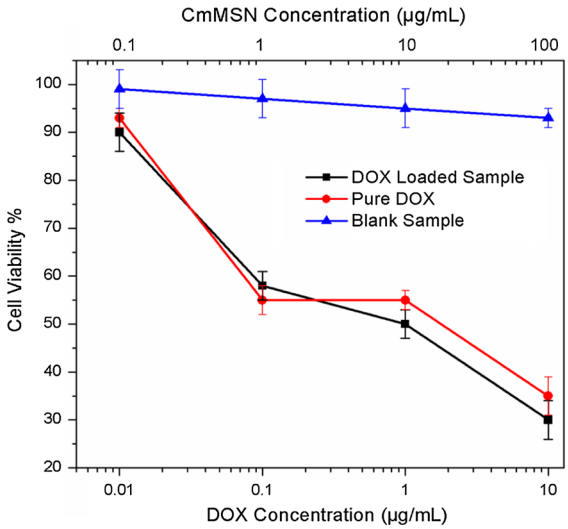

Fig. 12 Cell survival assay of HeLa cells: for blank ~MSN, pure DOX, and DOX@ ~MSN

Conclusion

In the present investigation, an efficient responsive carrier system has been successfully constructed by oppositely charged ionic interaction between polycations and anionic CmMSN. This intelligent system is efficient for storage and release of drug controlled by the pH. Moreover, this system with attractive features of high drug loading capacity, mild storage-release conditions, and stable mesostructure will be considered as an interesting alternative to the polymeric delivery system. The well-defined core–shell nanospheres were confirmed by the results from SEM observation, FTIR spectra, BET, and Nitrogen-desorption isotherm. In-vitro cytotoxicity of ~MSN to HeLa cells was investigated by MTT assay. The cumulative release of ~MSN showed that a low leakage at pH 6.5 with only 10 % amount was released after 4 h while significantly enhanced up to near about 80.2 % at pH 4.5. These results demonstrated that the drug release from the ~MSN was pH-responsive apparently. More significantly, artificial molecular gates around pores switched on and off by the pH value are of great importance for other potential applications including sensors and molecular machines.

Acknowledgments Authors would like to acknowledge funding support from Department of Science and Technology (DST), Government of India and FA5209-11-P-0160, ITC-PAC Fund Support.

References

Angelos S, Yang YW, Patel K, Stoddart JF, Zink JI (2008) pH-responsive supramolecular nanovalves based on cucurbit uril[6]pseudorotaxanes. Angew Chem Int Ed 47:2222–2226

Aznar E, Marcos MD, Martinez-Manez R (2009) pH- and photo-switched release of guest molecules from mesoporous silica supports. J Am Chem Soc 131:6833–6843

Besseling NAM, Stuart MAC, Fokkink RG (1998) Formation of micelles with complex coacervate cores. Langmuir 14:6846–6849

Carmen AL, Angel C, Schneider HJ, Mohsen S (2013) Smart materials for drug delivery. Royal Society of Chemistry, London

Chen HR, Shi JL, Li YS, Hua ZL, Chen HG, Yan DS (2003) Hollow mesoporous silica nanoparticles for intracellular delivery of fluorescent dye. Adv Mater 15:1078

Gao Q, Xu Y, Wu D, Sun YH, Li XA (2009) pH-responsive drug release from polymer-coated mesoporous silica spheres. J Phys Chem 113:12753–12758

Hernandez R, Tseng HR, Wong JW, Stoddart JF, Zink J (2004) An operational supramolecular nanovalve. I J Am Chem Soc 126:3370

Hong CY, Li X, Pan CY (2009) Fabrication of smart nanocontainers with a meso-porous core and a pH-responsive shell for controlled uptake and release. J Mater Chem 19:5155–5160

Hu Y, Chen Y, Chen Q, Zhang LY, Jiang XQ, Yang CZ (2005) Synthesis and stimuli-responsive properties of chitosan/poly(acrylic acid) hollow nanospheres. Polymer 46:12703–12710

Jiao Y, Guo J, Shen S, Chang B, Zhang Y, Jiang X, Yang W (2012) Synthesis of discrete and dispersible hollow mesoporous silica nanoparticles with tailored shell thickness for controlled drug release. J Mater Chem 22:17636–17643

Khaled A, Guo S, Li F, Guo P (2005) Controllable self-assembly of nanoparticles for specific delivery of multiple therapeutic molecules to cancer cells using RNA nanotechnology. Nano Lett 5(9):1797–1808

Lai CY, Trewyn BG, Jeftinija DM, Jeftinija K, Xu S, Jeftinija S, Lin VS-Y (2003) A mesoporous silica nanosphere-based carrier system with chemically removable CdS nanoparticle caps for stimuli-responsive controlled release of neurotransmitters and drug molecules. J Am Chem Soc 125:4451

Lee CH, Cheng SH, Huang IP, Souris JS, Yang CS, Mou CY, Lo LW (2010) Intracellular pH-responsive mesoporous silica nanoparticles for the controlled release of anticancer chemotherapeutics. Angew Chem Int 49:8214

Liao PH, Liu R, Liu JK, Feng PY (2011) Responsive polymer-based mesoporous silica as a pH-sensitive nanocarrier for controlled release. Langmuir 27:3095–3099

Lim MH, Blanford CF, Stein A (1998) Synthesis of ordered microporous silicates with organosulfur surface groups and their applications as solid acid catalysts. Chem Mater 10:467

Liu FT, Eisenberg A (2003) Preparation and pH triggered inversion of vesicles from poly(acrylicacid)-block-polystyrene-block-poly(4-vinyl pyridine). J Am Chem Soc 125:15059–15064

Liu TY, Hu SH, Liu TY, Liu DM, Chen SY (2006) Magnetic-sensitive behavior of intelligent ferrogels for controlled release of drug. Langmuir 22:5974–5978

Mal NK, Fujiwara M, Tanaka Y, Taguchi T, Matsukata M (2003) Photo controlled release of guest molecules from coumarin modified MCM-41. Chem Mater 15:3385

Manzano M, Vallet-Regi M (2010) Advanced drug delivery vectors with tailored surface properties made of mesoporous binary oxides submicronic spheres. J Mater Chem 20:5593

Medeiros SF, Santos AM, Fessi H, Elaissari A (2011) Stimuli-responsive magnetic particles for biomedical applications. Int J Pharm 403:139–161

Meng HA, Xue M, Xia TA, Zhao YL, Tamanoi F, Stoddart JF, Zink JI, Nel AE (2010) Autonomous in vitro anticancer drug release from meso-porous silica nanoparticles by pH-sensitive nanovalves. J Am Chem Soc 46:12690–12697

Mishra SB, Pandey H, Pandey AC (2013) Nanosuspension of Phyllanthus amarus extract for improving oral bioavailability and prevention of paracetamol induced hepatotoxicity in Sprague–Dawley rats. Adv Nat Sci 4:1–6

Moghimi SM, Hunter AC, Murray JC (2001) Long-circulating and target-specific nanoparticles: theory to practice. Pharmacol Rev 53(21):283–318

Mou CY, Lee CH, Lo LW, Yang CS (2008) Synthesis and characterization of positive-charge functionalized mesoporous silica nanoparticles for oral drug delivery of an anti-inflammatory drug. Adv Funct Mater 18:3283

Pandey H, Parashar V, Parashar R, Prakash R, Ramteke P, Pandey AC (2011) Controlled drug release characteristics and enhanced antibacterial effect of graphene nanosheets containing gentamicin sulphate. Nanoscale 3:4104–4108

Park YJ, Nah SH, Lee JY, Jeong JM, Chung JK, Lee MC, Yang VC, Lee SJ (2003) Surface-modified poly(lactide-*co*-glycolide) nanospheres for targeted bone imaging with enhanced labeling and delivery of radioisotope. J Biomed Mater Res 67A:751–760

Pere-Quintanilla D, Sanchez A, del Hierro I, Fajardo M, Sierra I (2007) Organic–inorganic hybrid mesoporous silicas and their applications in environmental protection. J Colloid Interface Sci 313:551

Qiu Y, Park K (2001) Responsive polymeric delivery systems. Adv Drug Deliv Rev 53:321–339

Radu DR, Yu LC, Ksenija J, Rowe EW, Jeftinija S, Lin VS-Y (2004) A polyamidoamine dendrimer-capped mesoporous silica nanosphere-based gene transfection reagent. J Am Chem Soc 126(41):13216–13217

Rao YVS, de Vos DE, Jacobs PA (1997) 1,5,7-Triazabicyclo[4.4.0]dec-5-ene Immobilized in MCM-41: a strongly basic porous catalyst. Angew Chem Int 36:2661–2663

Schmaljohann D (2006) Thermo- and pH-responsive polymers in drug delivery. Adv Drug Deliv Rev 58:1655–1670

Slowing II, Vivero-Escoto JL, Wu CW, Lin VSY (2008) Mesoporous silica nanoparticles as controlled release drug delivery and gene transfection carriers. Adv Drug Deliv Rev 60(11):1278

Stuart MAC, Besseling NAM, Fokkink RG (1998) Formation of micelles with complex coacervate cores. Langmuir 14:6846–6849

Stuart M, Huck W, Genzer J, Müller M, Ober C, Stamm M (2010) Emerging applications of stimuli-responsive polymer materials. Nat Mater 9:101–113

Sun JT, Hong CY, Pan CY (2010) Fabrication of PDEAEMA-coated mesoporous silica nanoparticles and pH-responsive controlled release. J Phys Chem 114:12481–12486

Tang H, Guoa J, Sunb Y, Changa B, Renb Q, Yanga W (2011) Facile synthesis of pH sensitive polymer-coated mesoporous silica nanoparticles and their application in drug delivery. Int J Pharm 421:388–396

Tasciotti E, Liu X, Bhavane R, Plant K, Price K, Cheng MM-C, Decuzzi P, James M, Robertson F, Ferrari M (2008) Mesoporous silicon particles as a multistage delivery system for imaging and therapeutic applications. Nat Nanotechnol 3:151–157

Trewyn BG, Giri S, Slowing II, Lin VS, Victor SY (2007) Mesoporous silica nanoparticle based controlled release, drug delivery, and biosensor systems. Chem commun 31:3236–3245

Vallet-Regi M, Ramila A, Perez-Pariente J (2001) Mesoporous silica-based nanomaterials for drug delivery: evaluation of structural properties associated with release rate. Chem Mater 13:308

Yang Q, Wang S, Fan P, Wang L, Di Y, Lin K, Xiao F (2005) pH-responsive carrier system based on carboxylic acid modified mesoporous silica and polyelectrolytefor drug delivery. Chem Mater 17:5999–6003

Yoo H, Pak J (2013) Synthesis of highly fluorescent silica nanoparticles in a reverse microemulsion through double-layered doping of organic fluorophores. J Nanopart Res 15:1609

Zhao YL, Li ZX, Kabehie S, Botros YY, Stoddart JF, Zink JI (2010) pH-operated nanopistons on the surfaces of mesoporous silica nanoparticles. J Am Chem Soc 132: 13016–13025